Pergamon

PII: S0022-3697(96)00068-6

J. Phys. Chem Solids Vol 58, No. 2, pp. 345–352, 1997

0022-3697/97 $17.00 + 0.00

ELECTRONIC STRUCTURES OF FeS AND FeS_2: X-RAY ABSORPTION SPECTROSCOPY AND BAND STRUCTURE CALCULATIONS

M. WOMES†, R. C. KARNATAK†, J. M. ESTEVA†, I. LEFEBVRE‡, G. ALLAN‡, J. OLIVIER-FOURCADE§ and J. C. JUMAS§

†Laboratoire de Spectroscopie Atomique et Ionique (URA 775 CNRS), Université Paris-Sud, Bâtiment 350, F-91405 Orsay Cédex, France

‡Institut Supérieur d'Electronique du Nord, 41 Boulevard Vauban, F-59046 Lille Cédex, France

§Laboratoire de Physicochimie des Matériaux Solides (URA D0407 CNRS), Université Montpellier II, Sciences et Techniques du Languedoc, Place E. Bataillon, F-34095 Montpellier Cédex 5, France

(*Received* 24 *May* 1995; *accepted in revised form* 19 *March* 1996)

Abstract—The band structures of FeS and FeS_2 including the S 3*s* and 3*p* and the Fe 3*d* and 4*s* states are calculated in the tight-binding approach. In the case of FeS, magnetic ordering is taken into account. The Fe *K*, Fe $L_{2,3}$, and S *K* X-ray absorption edges have been recorded and are discussed in terms of the calculated band structures. The three absorption edges and the corresponding partial density of states (PDOS) in the conduction band are presented on a common relative energy scale for both compounds. This allows an interpretation of those structures in the spectra which correspond to bands not accessible by the calculation (particularly those derived from Fe 4*p* states). It is shown that the method of using band structure calculations together with a maximum number of absorption edges of a compound allows to describe conduction bands up to higher electronic levels and gives a detailed interpretation of X-ray absorption spectra.

Keywords: A. chalcogenides, C. XAFS, D. electronic structure.

1. INTRODUCTION

The two simplest binary iron sulfides, FeS (troilite) and FeS_2 (pyrite), have been the object of several theoretical and experimental studies [1–5]. One of the main interests of previous investigations was to establish a model of the band structures of these compounds in order to understand their optical, electrical and magnetic properties, which differ considerably. FeS, which can be written as $Fe^{2+}S^{2-}$ has a hexagonal structure [6] and is antiferromagnetic at room temperature [7]. FeS_2, on the other hand, is to be considered as $Fe^{2+}(S_2)^{2-}$. It is diamagnetic at room temperature due to the low spin configuration $3d(t_{2g})^6(e_g)^0$ of Fe, and its structure is of the cubic rocksalt type [8]. The most commonly used theoretical approach in the case of FeS_2 is that of the molecular cluster method [1, 2]. This approach seems to be well suited for FeS_2 and leads to results comparable to those obtained by other methods [3–5]. The band structure of FeS, however, can not be calculated by considering a single (Fe_6^{10-})-cluster, since this method neglects magnetic coupling between iron atoms. This difficulty might explain the present lack of theoretical work on FeS which takes into account magnetic ordering effects.

Among the experimental techniques used to study band structures, X-ray absorption spectroscopy (XAS) plays a predominant part since it is particularly well suited to getting insight into the partial density of unoccupied states in the conduction band, independently for each element contained in the compound. Sugiura and co-workers were the first to record S *K* ($1s \rightarrow 3p$) edge and Fe *K* ($1s \rightarrow 4p$) edge absorption spectra of iron sulfides [9–11]. The first multiple scattering calculation of the S *K* edge absorption spectrum of FeS was performed by Kitamura *et al.* [12], which allowed a detailed interpretation of the experimental data. However, a complete picture of the FeS and FeS_2 band structures could not be derived from these results due to the fact that the Fe L_3 ($2p_{3/2} \rightarrow 3d, 4s$) absorption edges were not investigated due to non-availability of appropriate reflecting crystals in the domain of Fe *L* edges.

The aim of this paper is to establish the band structures of FeS and FeS_2 by theoretical calculation up to an energy of 10 eV above the Fermi level and to compare them with results obtained from XAS. To this end, theoretical densities of states are used to superpose XAS spectra on a common energy scale. This aim is achieved by considering first the features

up to about 5 eV above the Fermi level, which can be described precisely by theoretical densities. Then this superposition is used to describe spectral features beyond +5 eV. In this way we arrive at a fully coherent description of empty states within 10 eV above the Fermi level.

The tight-binding method is chosen to calculate the partial densities of states for both compounds because of the complex atomic structure of FeS and its large number of atoms per unit cell (12 Fe and 12 S). In the case of FeS its magnetic structure is taken into account. The tight-binding method uses the linear combination of atomic orbitals (LCAO) theory. In solid state physics, one is generally interested in the study of the electronic properties of materials in a small region of energy close to that of the valence electrons. The LCAO development of wave functions is limited to the valence and/or conduction orbitals which are energetically close to the valence band. In the present case, for simplicity and precision, the calculations are performed by using only low energy valence Fe 3*d*, 4*s* and S 3*s*,3*p* orbitals. Considering the precision requirements, the calculations are not extended to higher energy Fe 4*p* excited states.

On the experimental side, XAS has been chosen since it allows to probe independently the iron and sulfur derived states in the conduction band. By studying the Fe *K*, Fe L_3, and S *K* X-ray absorption near edge structures (XANES) which correspond respectively to Fe 4*p*, Fe (3*d*,4*s*) and S 3*p* states, we obtain informations on all relevant states composing the conduction band.

Our paper is organized as follows: Section 2 will briefly summarize some structural details of FeS and FeS_2. Then Section 3 will deal with the calculation of band structure in the tight-binding approach, while in Section 4 the experimental details will be described. In Section 5 we shall present the results of our band structure calculations for both compounds. The S *K*, Fe *K* and Fe L_3 edges will be discussed in detail with reference to the calculated partial densities of states (PDOS). The last Section (6) will be devoted to the conclusion which we obtain from a comparative study of the band structure and X-ray absorption edges of these compounds by the superposition of the spectra and theoretical PDOS on a common relative energy scale.

2. CRYSTAL STRUCTURES

The troilite structure can be derived from the NiAs type. Both Fe and S form slightly distorted close-packed hexagonal sublattices [6]. The Fe sublattice may be considered as being composed of contracted and expanded triangles. The contracted triangles push the anions situated above them somewhat away in the *z* direction perpendicular to the anion planes, while the expanded triangles allow the anions to enter somewhat more into the iron planes. As a consequence, we find five different Fe–S distances in the FeS_6-octahedra varying from 2.35 to 2.64 Å, with a mean Fe–S distance of 2.50 Å. The magnetic moments, pointing along the c axis, are parallel within each (0001) plane and antiparallel to those in neighbouring planes [7].

The pyrite structure is of the cubic face-centred NaCl-type with $(S–S)^{2-}$ pairs on the anion sites. The axes of these pairs are directed along the four [111] directions of the cube [8]. The S–S distance in these pairs is 2.14 Å. The Fe ions are situated in the centre of an octahedron formed by six nearest-neighbour sulfur anions at a distance of 2.26 Å. As all anions are slightly displaced from the corners of the cube in [111] direction, the FeS_6-octahedra are distorted and may be considered as being compressed in [111] direction.

3. METHOD OF CALCULATION

Our aim is to obtain the electronic structure of both FeS and FeS_2 by using the same theoretical method in order to compare them. The tight binding method allows to take into account the complex atomic structure of FeS and its magnetic character. In this method, the wave function is expressed as a linear combination of atomic orbitals (LCAO theory). A minimal basis set including *s* and *p* states for S and *s* and *d* states for Fe is used. The calculation of the Hamiltonian matrix elements has been described in more detail elsewhere [13]. The interaction parameters only take into account one-electron effects. The partial densities of states are calculated by integrating the obtained band structure over the Brillouin zone using "special points" [14].

The magnetic interaction in FeS has been taken into account in the following way [15, 16]. The magnetism comes from different populations of the Fe *d* spin up and spin down states ($n\uparrow$ and $n\downarrow$) on an iron atom. This corresponds to an energy change which may be written within the Hartee–Fock model as

$$E_i\uparrow = E_d^0 - V_i$$

$$E_i\downarrow = E_d^0 + V_i$$

where E_d^0 is the atomic energy and V_i the electronic exchange term on the *i*th iron site. Thus $(n\uparrow - n\downarrow)$ can be obtained by integrating the local density of states on site *i*, which, in turn, allows the calculation of the one-spin susceptibility matrix elements

$$\frac{\chi_{ij} = \partial(n\uparrow - n\downarrow)_i}{\partial V_j}$$

Its highest eigenvalue χ_M corresponds to the most stable spin configuration. We find $\chi_M = 4.39\,eV^{-1}$. This susceptibility, associated to the intraatomic Coulomb term which is generally assumed to be $U = 0.6\,eV$ [16], satisfies Stoner's condition $\chi_M U > 1$. The Hartree–Fock model also assumes that

$$V_i = U\frac{(n\uparrow - n\downarrow)_i}{2}$$

To simplify and to get a self consistent solution we only consider the electronic spin configuration proportional to the susceptibility matrix eigenvector corresponding to χ_M. The spin wave of this selfconsistent solution is oriented along the crystallographic c axis with slightly different magnetisations for iron atoms belonging to the same plane. This magnetic ordering also opens a weak gap of about 0.2 eV in the Fe $3d$ density of states.

4. EXPERIMENTAL

The samples were synthesized by heating stoichiometric mixtures of the pure elements in evacuated silica tubes for several days up to 800°C and 450°C for FeS and FeS_2 respectively. X-ray powder diffraction and ^{57}Fe Mössbauer spectroscopy revealed that the reactions had been completed leading to the pure troilite and pyrite phases.

The XAS measurements were carried out at LURE, Orsay. The Fe K edge spectra were recorded at DCI storage ring in the transmission mode using a double crystal monochromator. Two parallel Si (311) crystals were used as monochromators and yielded a resolution of 1.7 eV. The absorption screen was placed between two ion chambers which were used to measure the incident (I_0) and transmitted (I) intensities. The absorption screens were prepared by dusting the finely ground polycrystalline powders, sieved to 20 μm onto adhesive tape. The Fe L_3 and S K edges were measured at Super ACO storage ring in the total electron yield mode using a "channeltron" detector, on finely ground powder samples spread on an adhesive tape. In the case of the S K edge, a double crystal monochromator with two InSb crystals allowing a resolution of 1 eV was used. For the Fe L_3 edge a monochromator equipped with an organic crystal, potassium acid phthalate (KAP), preceded by a carbon–tungsten multilayer array giving a resolution of about 1.5 eV was used. The different monochromators were calibrated as follows: for the Fe K edge the point at half height of the absorption step maximum of Fe metal was set to 7111.0 eV [17]. For the S K edge the maximum of the white line of FeS_2 was set to 2472.1 eV [10]. In the case of the Fe L_3 edge, the absorption maximum of the white line of Fe_2O_3 was set to 708.5 eV.

The absorption spectra were obtained by step scanning with an energy step of 0.2 eV. They were corrected for a linear base line which was fitted to the pre-edge part of each spectrum. Finally, the spectra were normalized with respect to the point of maximal absorption. Throughout this paper the positions of white lines correspond to their intensity maximum point and the positions of arctangent like steps to their inflection point.

5. RESULTS AND DISCUSSIONS

5.1. *Comparison between theory and experiment*

In this paragraph we will present the results of our band structure calculations for both compounds and discuss the experimental spectra with reference to the calculated band structures. For a comparison with the experimental spectra, the theoretical PDOS were convoluted with a 1 eV wide Gaussian function. This width was chosen so as to keep visible the details of PDOS. Figure 1 shows the partial densities of the S $3s$ and $3p$ states together with those of the Fe $3d$ and $4s$ states of FeS_2, while Fig. 2 shows the corresponding PDOS of FeS. In the case of FeS_2, we find the sulfur $3s$ bands which are due to the S–S interaction, at about −17 and −13 eV with respect to the Fermi energy E_F.

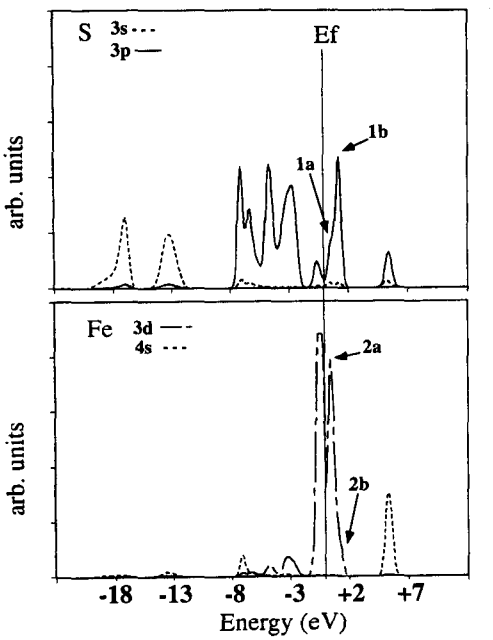

Fig. 1. Theoretical partial density of S($3p$), S($3s$), Fe($4s$) and Fe($3d$) states for FeS_2. These curves are obtained by broadening the theoretical densities by a 1 eV wide Gaussian function. The vertical line E_F indicates the position of the Fermi level.

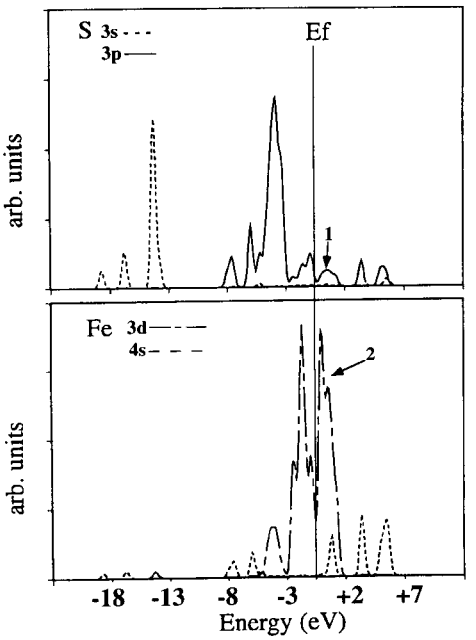

Fig. 2. Theoretical partial density of S(3*p*), S(3*s*), Fe(4*s*) and Fe(3*d*) states for FeS. These curves are obtained by broadening the theoretical densities by a 1 eV wide Gaussian function. The vertical line E_F indicates the position of the Fermi level.

The S *p* bands lie in the −8 to −2 eV energy range. The small peak just below E_F represents S *p* states hybridized with the filled Fe 3*d* (t_{2g}) band. We observe at about 1 eV above E_F a strong peak (labelled 1b) due to S *p* states with a shoulder (1a) on its low energy side. This peak represents an empty band of S 3*p* antibonding states caused by the S–S bonds, while the shoulder, 0.7 eV below the maximum, is due to S 3*p* orbitals hybridized with empty Fe 3*d* (e_g) states. The Fe 3*d* density of states shows a corresponding weak shoulder (2(b)) owing to hybridization with S 3*p* states about 0.7 eV above its maximum (2(a)), the latter originating from the empty 3*d* (e_g) band. Finally, S 3*p* states hybridized with Fe 4*s* states are observed at about 5.5 eV above E_F. Corresponding peaks are found in both the S 3*p* and the Fe 4*s* PDOS.

In the case of FeS (Fig. 2), the S 3*s* bands lie between −19 to −13 eV below the Fermi level. This is followed by a band between −8 eV and E_F which is of mainly S 3*p* character hybridized with Fe 3*d* (t_{2g}) states. Above, E_F we find three peaks at 1 eV, 4 eV and 6 eV, the first of which, labelled 1, is predominantly mixed with Fe 3*d* states and the latter two with Fe 4*s* states. Owing to the absence of S–S bonds in FeS no empty S 3*p* band is found. The Fe 3*d* PDOS reveals five peaks between −2 eV and +2 eV, three peaks below and two above E_F, the splitting between the two latter ones, labelled 2, is 0.7 eV. The Fe 4*s* bands, situated 1.5, 4, and 6 eV above E_F, coincide with corresponding S 3*p* bands.

Let us now turn to the experimental results. The left panel of Fig. 3 shows the S *K* absorption spectra of both compounds reflecting transitions from the S 1*s* core state to unoccupied states of S 3*p* character. The positions of all features discussed below are given in Table 1. The second derivatives of the curves are shown on the right panel. By comparison with the PDOS, we identify the white line labelled "A" in the spectrum of FeS_2 as predominantly due to transitions to the antibonding S 3*p* band (1b in Fig. 1). The low energy shoulder seen in the PDOS (1a), which is due to S 3*p*–Fe 3*d* hybridization, is not resolved either in the spectrum or in its second derivative. Point C may be attributed to transitions to S *p* states hybridized with Fe 4*s* states, although the energy separation A–C of

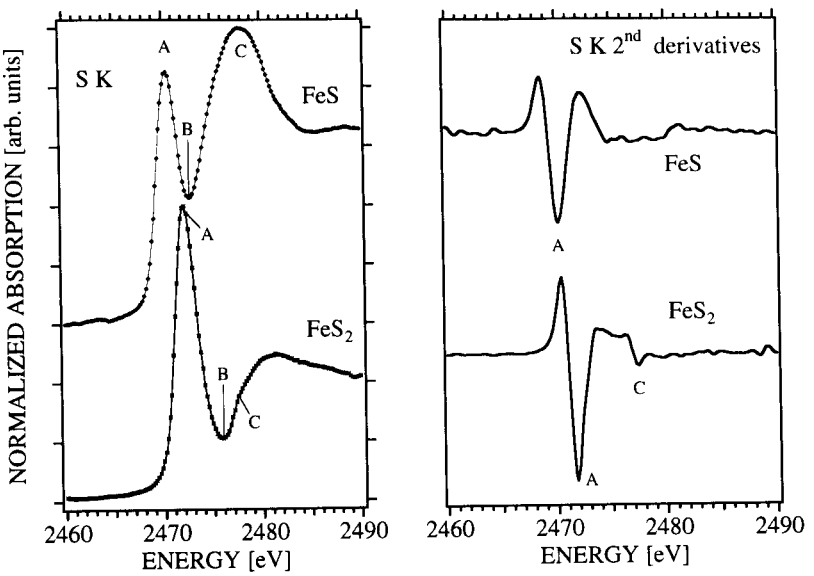

Fig. 3. Sulfur *K* absorption edges (left panel) and their second derivatives (right panel) of FeS and FeS_2.

Table 1. Peak position (in eV) of the Fe K, Fe L_3 and S K edges as labelled in Figs 3–5

	A	B	C	D	E
FeS Fe K	7110.7	7109.0	7107.1	7103.0	—
Fes_2 Fe K	7110.4	7108.9	—	7103.2	7114.5
FeS S K	2470.4	2472.8	2478	—	—
FeS_2 S K	2472.1	2476.1	2477.6	—	—
FeS Fe L_{23}	706.9	708.3	—	719.7	721.9
FeS_2 Fe L_{23}	707.3	708.3	712.7	719.7	721.1

5.5 eV derived from the second derivative (cf. Table 1) is somewhat higher than the 4.4 eV obtained from the calculation. A better agreement with theory is obtained by taking the onset of transitions to S p states in the continuum at point B, the relative minimum between A and C, lying 4.0 eV above A. The superposition of the S K curve on a common relative energy scale with the Fe K and L_3 edges discussed in the next section will support this interpretation. In FeS no S–S bonds are present and, therefore, the white line "A" represents only transitions to S 3p states mainly mixed with Fe 3d orbitals. Its intensity with respect to the absorption jump corresponding to pure atomic absorption above 2485 eV is thus strongly reduced as compared to that for FeS_2. As for FeS_2, we may identify point B as the onset of transitions to S 3p states hybridized with Fe 4s states, since the separation A–B of 2.4 eV agrees well with the 2.2 eV between the maximum of peak 1 in Fig. 2 and the second of the three S 3p–Fe 4s peaks. The meaning of the minimum B and the peak C will, however, be more evident from the superposition of all edges shown in the next section. Our spectra agree in shape with those published previously by Sugiura [10]. The white lines of our spectra are 50% narrower that those reported in Ref. [10].

Let us now turn to the Fe $L_{2,3}$ edges. It is well known that the L edges of transition metals usually cannot be interpreted in terms of a one-electron picture such as, for example, the one used in the present calculations. 3d–3d Coulomb interactions lead to a localization of the 3d electrons and cause a breakdown of one-electron theory. Ligand-to-metal charge transfer can modify the spectral shape and cause additional satellite structures which are, however, weaker than those observed in 2p X-ray photoemission spectra. The 2p absorption spectra are, therefore, usually interpreted in terms of atomic multiplets including 2p–3d and 3d–3d interactions (see, e.g., Ref. [18]) and ligand-to-metal charge transfer effects [19]. Multiplet calculations also allow us to explain differences in shape between the L_2 and L_3 edge. However, several authors have pointed out that the 3d–3d two-particle interaction is rather weak in FeS_2 [20, 21] and that 3d electrons in this compound are rather delocalized. This fact should allow an interpretation of the 2p XAS in terms of a one-electron band theory. FeS is considered as being on the boundary between localized and delocalized 3d electrons [20], so that the question arises which of the two approaches, one- or two-particle theory, gives better results. We will now compare our experimental spectra with the PDOS of Figs 1 and 2 which are based on a one-electron approach.

The Fe $L_{2,3}$ edges of FeS_2 (Fig. 4) agree well in shape with those measured by van der Laan *et al.* [22]. The Fe L_3 white line of FeS_2 is expected to contain transitions to the empty 3d (e_g) band as well as to Fe 3d states hybridized with the S 3p band, as we see from the corresponding PDOS (Fig. 1). The second derivative of the spectrum shows that the white line consists of two peaks, A and B, separated by 1 eV, which agrees

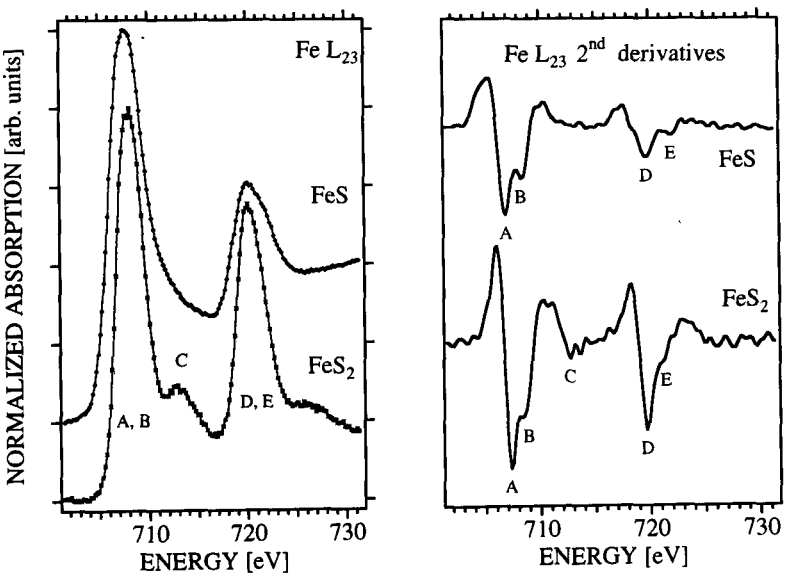

Fig. 4. Iron L_{23} absorption edges (left panel) and their second derivatives (right panel) of FeS and FeS_2.

well with the 0.7 eV given by the calculation. The small peak C about 5 eV above the maximum of the white line can be interpreted as a $2p \rightarrow 4s$ transition in agreement with the separation between Fe $3d$ and $4s$ states of 5.0 eV obtained from the PDOS. As the matrix elements of $2p \rightarrow 4s$ transitions are much smaller than those of $2p \rightarrow 3d$ transitions [23], the intensity of this peak is much smaller than would be expected from the PDOS. In the case of FeS, the calculation gives a separation of about 3 and 5 eV between the Fe $3d$ and the two highest Fe $4s$ states. In the FeS spectrum, the $4s$ states are not well resolved, but we observe an asymmetry on the high energy side of the white line and an increased full width at half maximum (FWHM) of 4.7 eV as compared to 3.7 eV observed in FeS_2. It can thus be concluded that the $2p \rightarrow 4s$ transitions in FeS are included on the high energy side of the while line. The $4s$ states are not resolved by the second derivative. However, we see that the second derivative shows two peaks A and B separated by about 1.4 eV. This value does not agree with the separation of 0.6 eV between the two peaks above E_F in the Fe $3d$ PDOS (labelled 2 in Fig. 2) and, therefore, these structures seem to have no equivalent in the one-electron band theory. Furthermore, we see from the positions of the structures A, B, D and E that the L_2 and L_3 edges of FeS differ considerably in shape while the agreement is better in the case of FeS_2. These points, the poor agreement with calculation and the differences in shape between L_2 and L_3 in the case of FeS indicate a stronger influence of two-electron correlations, in agreement with the more localized character of the $3d$ electrons in this compound as it follows from theoretical considerations [21].

Our spectra of the Fe K edges of both compounds, shown in Fig. 5, agree well in shape, but provide better signal-to-noise ratio than those published earlier [11]. This allows an evaluation of their derivatives in order to make more clearly visible the structures contained in the absorption edges. The Fe K edges are arctangent like step functions. We, therefore, chose the first derivatives rather than the second ones. The Fe K edge and its first derivative of FeS_2 show several features labelled A, B, D, E and R. Owing to the compression in [111] direction of the FeS_6 polyhedra in FeS_2 leading to a Fe site symmetry of C_{3i} [8], the Fe $4p$ states are split into an A_{1u} singlet and an E_u doublet, with the singlet orbital, pointing in [111] direction, being shifted to higher energies. We, therefore, interpret the features A and B as transitions to the doublet and the singlet respectively, in analogy with similar effects observed at the Cu K-edge of copper oxides [24]. The separation between the two peaks is 1.5 eV. The same distortion leads to an admixture of Fe $4p$ orbitals to the Fe $3d$ states [25, 26] and gives rise to the pre-peak labelled D in Fig. 5. Feature R is interpreted as a multiple scattering resonance of Fe p-like states in the continuum. The origin of peak E will be discussed in the next section.

In FeS, we find FeS_6 polyhedra with five different Fe–S distances [6], the degeneracy of the $4p$ states is thus completely lifted. Consequently, three structures, labelled A, B and C and separated by 1.7 and 1.6 eV respectively, are seen in the main absorption step. The interpretation of the features D and R is the same as described for FeS_2.

5.2. *Superpositions*

A clear picture of the conduction band emerges when we superimpose the calculated empty PDOS

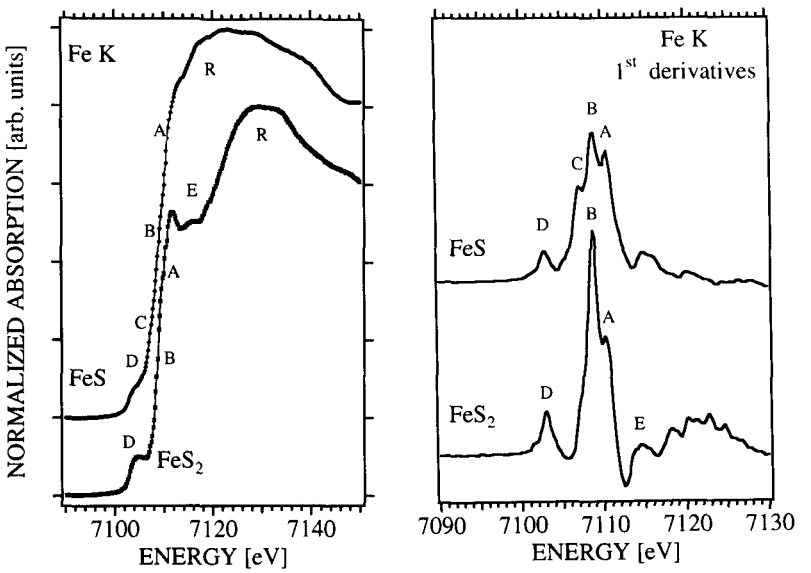

Fig. 5. Iron K absorption edges (left panel) and their first derivatives (right panel) of FeS and FeS_2.

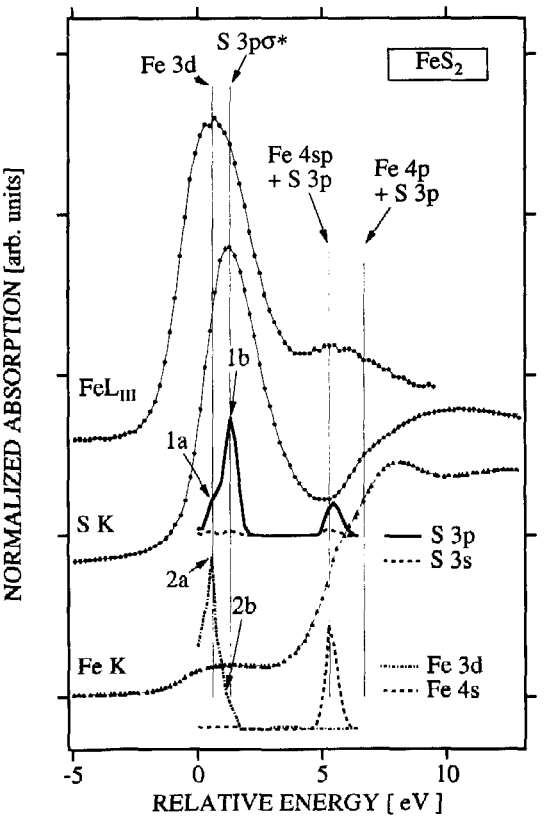

Fig. 6. Superposition of the Fe K, Fe L_3, S K edges and theoretical PDOS of FeS_2 on a common energy scale.

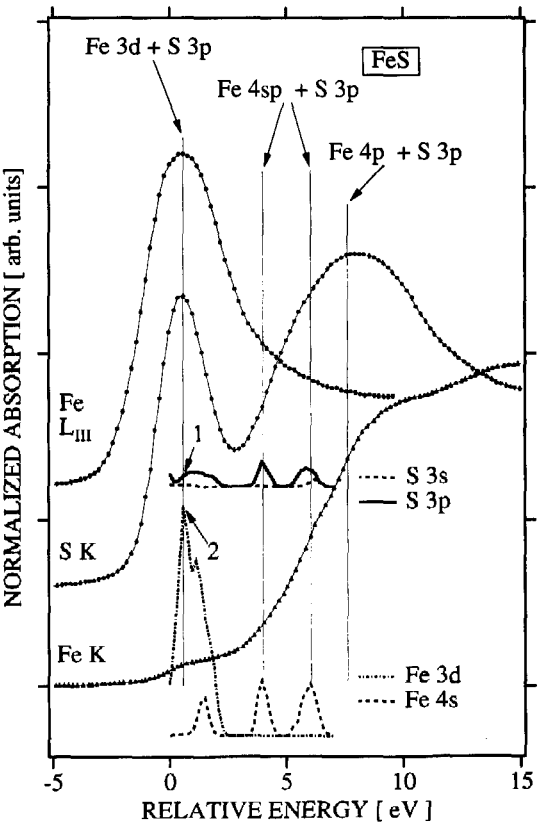

Fig. 7. Superposition of the Fe K, Fe L_3, S K edges and theoretical PDOS of FeS on a common energy scale.

above E_F and the experimental absorption edges of FeS_2 and FeS plotted on a relative energy scale. The calculated PDOS and the identification of the various structures in the absorption spectra as they were discussed in the preceding section, will now serve to superimpose, for each compound, the observed spectra and the corresponding PDOS above E_F. As we will see later, this approach extends the identification to higher vacant electronic states, such as Fe4p states, which are not accessible by the tight-binding method. We again normalize all spectra to have the same intensity at the point of maximum absorption. The origins of the energy scales have been taken at E_F.

Let us first consider FeS_2. In Fig. 6 we present Fe L_3, Fe K and S K edges of FeS_2 together with the vacant PDOS above E_F. In this figure, first the maxima of the Fe L_3 and S K edges were aligned to the maxima of the corresponding peaks 1b and 2a respectively of S 3p and Fe 3d PDOS. The maxima of the two white lines are thus separated by 0.7 eV to mimic the calculated separation between the Fe $3d(e_g)$ and S 3p bands. Peak D of the Fe K edge attributed to $1s \rightarrow 3d$ transitions in the preceding section is positioned with its maximum below the maximum of the Fe L_3 edge. In doing so we find coincidence of the small peak above the Fe 3d white line attributed to $2p \rightarrow 4s$ transitions, with point B of the S K edge assigned to the onset of transitions to S 3p states in the continuum and with the inflection point of peak B of the Fe K edge. The coincidence of all these points indicates that in this part of the conduction band the S 3p states are hybridized with Fe 4s and 4p states. This is in agreement with the calculation of Bullett [4] as well as our own and justifies our interpretation of B as the onset of transitions to S 3p states. Furthermore, we see that the inflection point of peak A of the Fe K edge coincides with shoulder C of the S K edge. It can, therefore, be concluded that the whole structure in the S K edge between 2475 and 2480 eV represents the S p states hybridized with Fe p states. Moreover, the peak E of the Fe K edge falls on the high energy tail of the S 3p structure C. From the present results, thus it seems that E represents a feature belonging to higher Fe p states hybridized with S orbitals in the conduction band rather than a part of the resonance structure R.

Figure 7 shows the superposition of the FeS spectra and the calculated PDOS. As the S 3p and the Fe 3d structures coincide in the PDOS, the maxima of the Fe L_3 and S K white lines were matched together with peak D of the Fe K edge at the same energy. The inflection points C, B and A of the Fe K edge are situated at 4.3, 6.0, and 7.6 eV above E_F respectively.

The first two of these peaks should approximately coincide with the two highest Fe 4*s* states seen in the Fe 4*s* PDOS. The tail on the high energy side of the Fe L_3 white line, which we attributed to Fe 4*s* states in the preceding section, falls effectively on the lower part of the Fe *K* absorption step. It can, therefore, be concluded that this part of the L_3 edge contains the Fe 4*s* states and that they are, in agreement with the calculated PDOS, not only hybridized with S 3*p* orbitals but also mixed with Fe 4*p* states. The low energy side of peak C of the S *K* edge coincides with the main absorption step of the Fe *K* edge over an energy range of about 5 eV. We, therefore, attribute peak C to transitions to S *p*-like states in the conduction band which are hybridized with Fe 4*sp* orbitals. The intensity of this peak might be enhanced by multiple scattering resonance effects in the continuum. Point B may be identified, in analogy to FeS_2, as the point marking roughly the onset of transitions to the S 3*p*–Fe 4*sp* band.

6. CONCLUSIONS

The PDOS close to the Fermi level of FeS and FeS_2 were calculated. The results of the calculation allowed an interpretation of the low energy features observed in the experimental Fe *K*, Fe L_3, and S *K* X-ray absorption edges of these compounds. Some structures corresponding to bands not included in our calculation have been identified by means of a superposition of the three edges and the corresponding PDOS on a common energy scale. This is especially the case for the structures seen in the Fe *K* edges which correspond to transition to 4*p* states. The S *K* edges agree well with the calculated band structure. Precise information on the accessible S 3*p* states and their hybridization with Fe 4*s* and Fe 4*p* states is obtained by superposition of all edges and the PDOS. The Fe L_3 edge of FeS_2 is well explained in terms of the PDOS, which in tight binding approach, correspond to the bottom of the conduction band. This is not the case for FeS. The fine structure seen in the second derivative does not agree with the calculation and should, therefore, be interpreted in terms of multiplet splittings and charge transfer effects in the initial and final states rather than in a one-electron picture. The different behaviour of FeS and FeS_2 is explained by the known delocalization of the Fe 3*d* electrons in FeS_2 and their comparatively more localized character in FeS.

The method of combining band structure calculations with a superposition of a maximum number of absorption edges of a compound proves to be a promising approach for a detailed interpretation of X-ray absorption spectra.

Acknowledgements—This research has been performed under an European research Network Programme (GDRE) 'Chalcogenides' initiated by the Centre National de la Recherche Scientifique (France). It has been financed in part by the 'Human Capital and Mobility' program of the European Communities.

REFERENCES

1. Tossell J. A., *J. Chem. Phys.* **66,** 5712 (1977).
2. Lauer S., Trautwein A. K. and Harris F. E. *Phys. Rev.* **B29,** 6774 (1984).
3. Khan M. A., *J. Phys. C: Solid State Phys.* **9,** 81 (1976).
4. Bullett D. W., *J. Phys. C: Solid State Phys.* **15,** 6163 (1982).
5. Folkerts W., Sawatzky G. A., Haas C., de Groot R. A. and Hillebrecht F. U. *J. Phys. C: Solid State Phys.* **20,** 4135 (1987).
6. Bertaut F., *Bull. Soc. Fr. Minér Crist.* **79,** 256 (1956).
7. Andresen A. F., *Acta Chem. Scand.* **14,** 919 (1960).
8. Finklea III S. L., Cathey L. and Amma E. L., *Acta Crystallogr. Sect. A* **32,** 529 (1976).
9. Sugiura C., Gohshi Y. and Suzuki I., *Phys. Rev.* **B10,** 338 (1974).
10. Sugiura C., *J. Chem. Phys.* **74,** 215, (1981).
11. Sugiura C., *J. Chem. Phys.* **80,** 1047 (1984).
12. Kitamura M., Sugiura C. and Muramatsu S. *Solid State Comm.* **67,** 313 (1988).
13. Wallart X., Nys J. P., Zeng H. S., Dalmai G., Lefebvre I. and Lannoo M., *Phys. Rev.* **B41,** 3087 (1990).
14. Chadi D. J. and Cohen M. L. *Phys. Rev.* **B8,** 5747 (1973).
15. Stoner E. C. *Proc. Roy. Soc. (London)* **A165,** 372 (1938); **A169,** 339 (1938).
16. Friedel J., *The Physics of Metals,* (Ed. J. M. Ziman). Cambridge University Press (1969).
17. Grunes L. A., *Phys. Rev.* **B27,** 2111 (1983).
18. de Groot F. M. F., Fuggle J. C., Thole B. T. and Sawatzky G. A., *Phys. Rev.* **B42,** 5459 (1990).
19. Okada K, Lotani A, *J. Electron Spectrosc. Relat. Phenom.* **62,** 131 (1993).
20. Wilson J. A., *Adv. Phys.* **21,** 143 (1972).
21. Bocquet A. E., Mizokawa T., Saitoh T., Namatame H. and Fujimori A. *Phys. Rev.* **B46,** 3771 (1992).
22. van der Laan G., Goedkoop J. P. and MacDowell A. A., *J. Phys.* **E20,** 1496 (1987).
23. Lerch P., Jarlborg T., Codazzi V., Loupias G. and Flank A. M., *Phys. Rev.* **B45,** 11481 (1992).
24. Guo J. and Ellis D. E., *Phys. Rev.* **B41,** 82 (1990).
25. Roe A. L., Schneider D. J., Mayer R. J., Pyrz J. W., Wydom J. and Que Jr L. *J. Am. Chem. Soc.* **106,** 1676 (1984).
26. Srivastava U. C. and Nigam H. L., *Coord. Chem. Rev.* **9,** 275 (1972).